water

MDPI

Article

Long Term Aquatic Vegetation Dynamics in Longgan Lake Using Landsat Time Series and Their Responses to Water Level Fluctuation

Wenxia Tan [1], Jindi Xing [1], Shao Yang [2,*], Gongliang Yu [3], Panpan Sun [2] and Yan Jiang [1]

[1] Key Laboratory for Geographical Process Analysis & Simulation of Hubei Province/College of Urban and Environmental Sciences, Central China Normal University, Wuhan 430079, China; tanwenxia@mail.ccnu.edu.cn (W.T.); jindixing@mails.ccnu.edu.cn (J.X.); jiangyan@mail.ccnu.edu.cn (Y.J.)
[2] School of Life Sciences, Central China Normal University, Wuhan 430079, China; wppxsun@hotmail.com
[3] Key Laboratory of Algal Biology, Institute of Hydrobiology, Chinese Academy of Sciences, Wuhan 430072, China; yugl@ihb.ac.cn
* Correspondence: yangshao@mail.ccnu.edu.cn

Received: 19 May 2020; Accepted: 30 July 2020; Published: 2 August 2020

Abstract: Aquatic vegetation in shallow freshwater lakes are severely degraded worldwide, even though they are essential for inland ecosystem services. Detailed information about the long term variability of aquatic plants can help investigate the potential driving mechanisms and help mitigate the degradation. In this paper, based on Google Earth Engine cloud-computing platform, we made use of a 33-year (1987–2019) retrospective archive of moderate resolution Landsat TM, ETM + and OLI satellite images to estimate the extent changes in aquatic vegetation in Longgan Lake from Middle Yangtze River Basin in China using the modified enhanced vegetation index, including emerged, floating-leaved and floating macrophytes. The analysis of the long term dynamics of aquatic vegetation showed that aquatic vegetation were mainly distributed in the western part of the lake, where lake bottom elevation ranged from 11 to 12 m, with average water depth of less than 1 m in spring. The vegetation area variation for the 33-year period were divided into six stages. In years with heavy precipitation, the vegetation area decreased sharply. In the following years, the area normally restored. Aquatic vegetation area had a significant negative correlation with the spring water level and summer water level. The results showed that aquatic vegetation was negatively affected when water depth exceeded 2.5 m in May and 5 m in summer. It is recommended that water depth remain close to 1 m in spring and close to 3 m in summer for aquatic vegetation growth. Our study provide quantitative evidence that water-level fluctuations drive vegetation changes in Longgan Lake, and present a basis for sustainable lake restoration and management.

Keywords: spatial-temporal dynamics; aquatic vegetation; water level fluctuation; Longgan lake; Google Earth Engine

1. Introduction

Wetlands play an important role in ecological services and socioeconomic services. As a basic component of wetland ecosystems, aquatic vegetation in shallow freshwater provide a variety of services, including improving water quality, maintaining aquatic ecosystem balance and providing food and habitats for many aquatic animals [1–3]. According to a recent investigation, decreasing aquatic vegetation are found in around 65.2% of the world lakes [4]. Due to rapid social and economic development during the past decades, dramatic variations in the distribution area of aquatic vegetation have been occurred in many lakes [5]. In addition, lake ecosystem have changed due to water level

management, nutrient input and global climate change [6,7]. In views of this, it is necessary to study the change trend of aquatic vegetation and its response to environmental factors.

Water-level fluctuation (WLF) has been well demonstrated as one of the core factors affecting biomass, diversity, composition and structure of vegetation, by causing variations in environmental factors for plant growth and germination, such as light, oxygen, temperature and nutrients etc. [8–10]. Based on the study of Great Lakes, Keddy and Reznicek concluded that during extremely high water periods, the dominant species were killed, thus creating gaps; however, many plant species and vegetation types regenerated from buried seeds during low water periods [11]. Therefore, fluctuating water levels generally increase the diversity of vegetation types and plant species. The influence of WLF on aquatic vegetation mainly manifests through variation of its amplitude and dynamic regime [12]. For example, by comparing the aquatic vegetation in two river-disconnected lakes (artificial water regime) and the river-connected lake (natural water regime), Zhang et al. [13] found that the plant species richness was highest in the disconnected lake with intermediate amplitude of WLFs, and lowest in the connected lake. The amplitude of WLFs was the most important factor in determining the distribution of lake-shore plants, followed by relative elevation and duration of submergence.

Macrophytes of different life forms response to WLF differently. By analyzing of the relationship between aquatic vegetation and WLFs in Taihu Lake from 1989 to 2010, Zhao et al. [14] found that water level from January to March had significant positive correlation with the coverage of emergent and floating-leaved vegetation, while had negative correlation with the coverage of submerged vegetation. Different macrophyte species of identical life form may also response to WLF differently. By treatment of three submerged macrophytes under different amplitude of WLF, Wang et al. [15] found *Hydrilla verticillata* exhibited more growth in static water, and *Elodea nuttallii* was inhibited by fluctuating water level treatments, while *Ceratophyllum demersum* became more abundant when water levels fluctuated.

Because aquatic vegetation in lakes and wetlands are often hard to reach, satellite images of Landsat and MODIS are employed for large scale and synoptic monitoring of lake vegetation [16–19]. Spectral indices (SIs), included various combinations of visible, near-infrared, and shortwave infrared bands, are widely used because their flexibility and capability for aquatic vegetation mapping. Villa et al. [20] and Villa et al. [21] summarized and compared several SIs for macrophyte mapping and concluded that the modified enhanced vegetation index (EVI) performed the best for three shallow freshwater bodies in different parts of Europe. The high temporal variability of aquatic vegetation in decades can offer pivotal information about the biological complexity of the lakes and wetlands. Szabó et al. [22] used Normalized Difference Vegetation Index (NDVI) for a 33-year long vegetation spread monitoring survey in an artificial lake in Hungary. Combining four vegetation indices (VI), Lopes et al. [23] studied the spatial and temporal vegetation changes within a coastal lagoon through Landsat imagery between 1984 and 2017. Google Earth Engine (GEE) [24], which is a cloud-based platform for earth science data analysis and visualization, is commonly used to study the dynamics of wetland land cover [25–27]. However, studies using GEE to investigate the long term variability of aquatic vegetation in shallow lakes are rarely found.

How water levels affect aquatic vegetation in natural lakes has been well studied. Hu et al. [28] took the use of time-series MODIS data to explore the relationship between wetland vegetation and factors linked with water-level fluctuations in Lake Poyang and Dongting. Using time-series of both MODIS and Landsat, the hydrological influence on the distribution and transition of wetland cover was studied [29]. Tan and Jiang [30], Wan et al. [31], You et al. [32], Zhang et al. [33] had also analyzed the relationship between wetland vegetation and water level for Lake Poyang and Dongting. However, Lake Poyang and Dongting are the only two lakes that are not dammed in the Yangtze river basin. All other lakes in the middle reaches of the Yangtze River are separated from the Yangtze River by dams and sluice gates. Thus, human interference is an important factor affecting lake water levels. As a national wetland reserve of China, Longgan Lake is an artificial regulated lake. However, the effects of human interference on water level to aquatic vegetation for Longgan Lake have been

little explored. It is helpful to explore the relationship between aquatic vegetation coverage and human regulated water levels with long-term data for lake ecological management. As submerged macrophytes disappeared from the lake in late 1990s, this study will only focus on the extent of emerged, floating-leaved and floating macrophytes.

Therefore, using GEE cloud-computing platform, this paper aimed to discuss the following issues: (1) to distinguish aquatic vegetation using medium-resolution Landsat satellite imagery; (2) to understand the long-term variation in the distribution area of aquatic vegetation over for more than 30 years; (3) to build relationships between aquatic vegetation and parameters associated with water-level fluctuations.

2. Materials and Methods

2.1. Study Area

Longgan Lake (29°52′–30°05′ N, 115°19′–116°17′ E), located in the middle reaches of the Yangtze River in central China, is a typical freshwater shallow lake covering an area of more than 300 km^2 in the junction of Hubei Province and Anhui Province (Figure 1). The lake is shaped like a shallow dish with lake bottom topography ranging between 10.5 m and 13.3 m (meters above sea level, reference to Wusong datum). The average spring water depth of the lake is 1–2 m, with a maximum summer depth of 3–5 m, varying from year to year. The climate is subtropical and the average annual precipitation in Longgan catchment is 1307 mm [34]. The western lakeshore was diked with three sluice gates (Tuohu, Yanjia, Hukou) as shown in Figure 1, which have been built to regulate river flow and control water levels since 1970s. The main inflows are from the northwestern catchment, and the outflow drains into the Yangtze River. Longgan Lake is one of the national nature reserves of wetland in China, serves as an important wetland habitat for many endangered waterbirds in the middle reaches of Yangtze River [35].

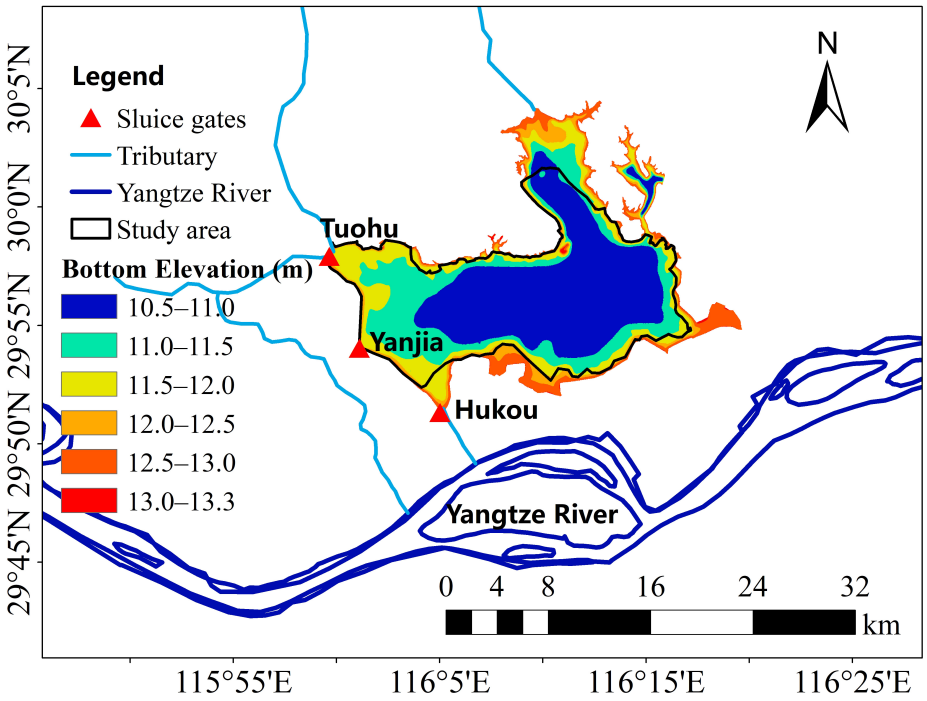

Figure 1. Location of Longgan Lake. The elevation of the lake bottom ranges between 10.5 m and 13.3 m (meters above sea level, reference to Wusong datum).

In 1993, the lake was at mesotrophic state and the aquatic vegetation coverage was up to 89.7%. Submerged macrophytes occupied the majority of the lake area, with a small area of emergent

and floating leaved macrophytes occupying the northwestern lakeshore. A total of 50 species of macrophytes were recorded in lake, including 15 species of submerged macrophytes, 7 species of floating-leaved macrophytes, 6 species of floating macrophytes and 22 species of emergent macrophytes or hygrophytes [36]. Since the late 1990s, submerged macrophytes almost disappeared, which was confirmed by our field investigation of 2017–2018.

2.2. Aquatic Vegetation Survey Data

In order to validate Landsat data, we conducted vegetation survey from 2017 to 2018 in the west part of Longgan Lake, where macrophytes were mostly distributed. The plant samples were collected for species identification. The plant community was investigated according to Braun-Blanquet methodology [37]. Georeferenced photographs were taken and the center coordinates were recorded with a handheld GPS. Vegetation coverage was estimated with position data recorded on site.

Quite different from the results of the survey of 1993, our survey found that the lake became highly eutrophic and vegetation coverage of the macrophytes decreased to 10%, indicating the wetland vegetation has degraded significantly. A total of 18 plant species were observed, including 4 species of submerged macrophytes, 5 species of floating-leaved macrophytes, 3 species of floating macrophytes and 6 species of emergent macrophytes or hygrophytes. The aquatic vegetation was dominated by emergent macrophyte *Zizania caduciflora*, floating-leaved macrophytes *Trapa litwinowii* and *Trapa bicornis* (Figure 2). Submerged macrophytes were distributed sparsely with very low biomass in the lake. In 2017, the vegetation was classified to 6 associations, i.e., *Trapa bicornis* Ass., *Nelumbo nucifera* Ass., *Euryale ferox* Ass., *Eichhornia crassipes* Ass., *Zizania caduciflora* + *Polygonum orientale* Ass., and *Trapa litwinowii* + *Eichhornia crassipes* + *Spirodela polyrhiza* Ass. In 2018, *Nelumbo nucifera* + *Trapa litwinowii* + *Euryale ferox* Ass. appeared near the north shoreline, but the *Trapa litwinowii* + *Eichhornia crassipes* + *Spirodela polyrhiza* Ass. disappeared (Figure 3).

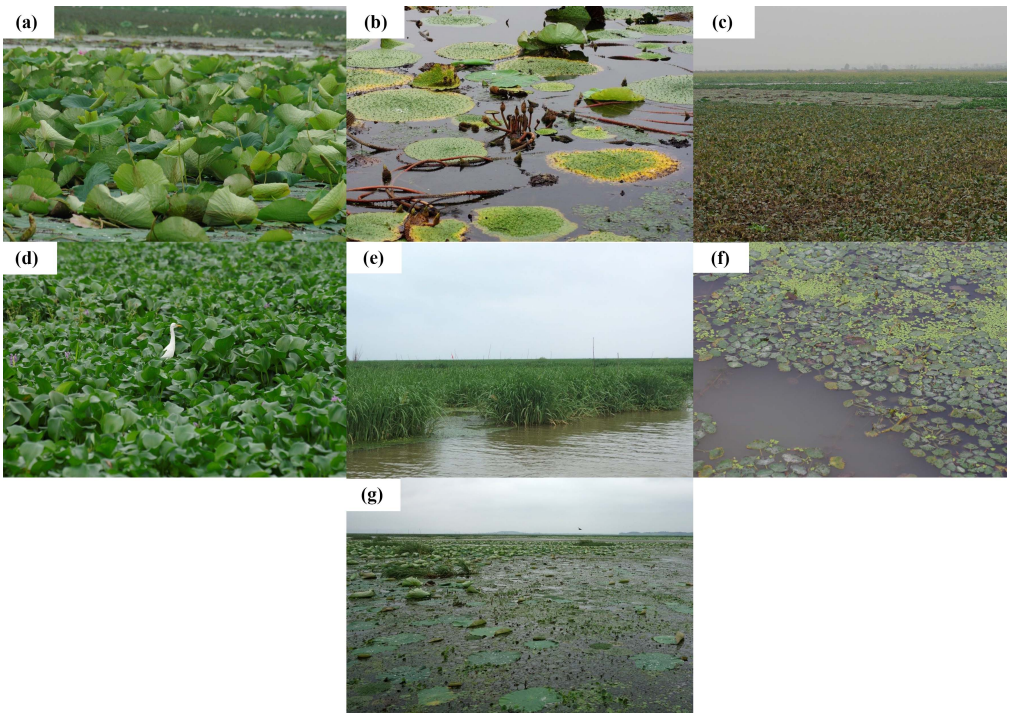

Figure 2. Photographs of aquatic vegetation observed in Longgan Lake. (**a**) *Nelumbo nucifera* Ass., (**b**) *Euryale ferox* Ass., (**c**) *Trapa bicornis* Ass., (**d**) *Eichhornia crassipes* Ass., (**e**) *Zizania caduciflora* + *Polygonum orientale* Ass., (**f**) *Trapa litwinowii* + *Eichhornia crassipes* + *Spirodela polyrhiza* Ass. and (**g**) *Nelumbo nucifera* + Trapa litwinowii + Euryale ferox Ass.

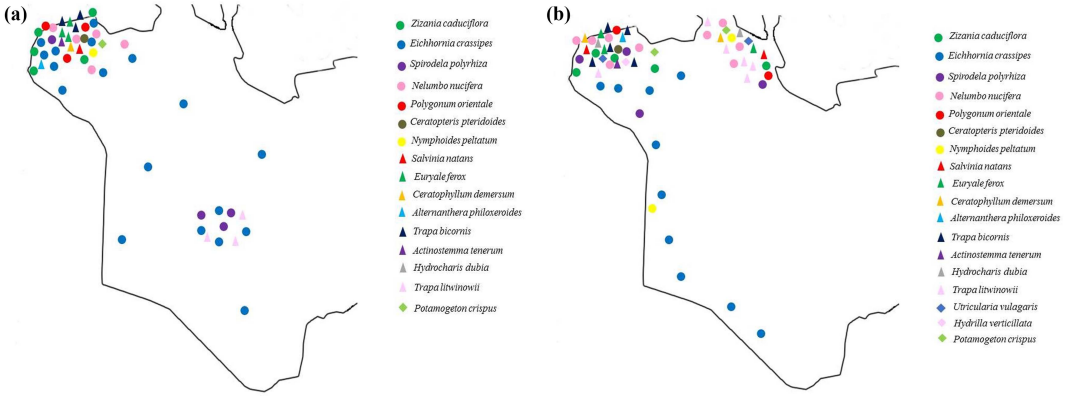

Figure 3. Distribution of macrophyte species in the western part of Longgan Lake for (**a**) September 2017 and (**b**) September 2018.

2.3. Satellite Data

All available Landsat top-of atmosphere (TOA) reflectance images for the WRS-2 footprints 121/39 and 122/39 in Google Earth Engine between 1987 and 2019 were used in this study, including Landsat 5 Thematic Mapper (TM), Landsat 7 Enhanced Thematic Mapper-plus (ETM+) and Landsat 8 Operational Land Imager (OLI) (as listed in Table 1). These datasets have a spatial resolution of 30 m. The images in late July were primarily selected to represent the vegetation cover extent of a year, because the vegetation coverage was highest during this time of a year. For years without cloud-free images in July, images in June and August were chosen instead. For Landsat 7 image in 2012, SLC-off gaps were filled with Phase 2 USGS Gap-Fill Algorithm [38].

Table 1. Temporal distribution of available Landsat images in Longgan Lake during 1987 to 2019.

Date	Sensor	Date	Sensor
27/08/1987	Landsat 5 TM	07/08/2003	Landsat 5 TM
26/06/1988	Landsat 5 TM	24/07/2004	Landsat 5 TM
15/07/1989	Landsat 5 TM	12/08/2005	Landsat 5 TM
09/07/1990	Landsat 5 TM	30/07/2006	Landsat 5 TM
26/06/1991	Landsat 5 TM	09/08/2007	Landsat 5 TM
23/07/1992	Landsat 5 TM	03/07/2008	Landsat 5 TM
10/07/1993	Landsat 5 TM	13/07/2009	Landsat 5 TM
04/07/1994	Landsat 5 TM	25/07/2010	Landsat 5 TM
05/06/1995	Landsat 5 TM	03/07/2011	Landsat 5 TM
25/07/1996	Landsat 5 TM	22/07/2012	Landsat 7 ETM +
29/08/1997	Landsat 5 TM	01/07/2013	Landsat 8 OLI_TIRS
08/07/1998	Landsat 5 TM	02/06/2014	Landsat 8 OLI_TIRS
02/07/1999	Landsat 5 TM	05/06/2015	Landsat 8 OLI_TIRS
05/07/2000	Landsat 5 TM	23/06/2016	Landsat 8 OLI_TIRS
24/07/2001	Landsat 7 ETM +	28/07/2017	Landsat 8 OLI_TIRS
11/07/2002	Landsat 7 ETM +	31/07/2018	Landsat 8 OLI_TIRS
		02/07/2019	Landsat 8 OLI_TIRS

High quality Sentinel-2 data with close acquisition dates as the corresponding Landsat images were used to validate the vegetation mapping results by the proposed method. Sentinel-2 have more than 10 bands, with spatial resolutions of 10–20 m. Moreover, a PROBA-V (Project for On-Board Autonomy-Vegetation) image of 26 June 2018 was also used in the discussion to show the aquatic vegetation cover difference between June and July 2018. Though PROBA-V has a lower spatial resolution (100 m) than that of Landsat, it was the only cloud free image that was found for June 2018 for Longgan Lake. PROBA-V is a satellite mission tasked to map land cover and vegetation growth on

a daily basis. The sensor collects data in three VNIR (red, blue and near-infrared) bands and one SWIR (short-wave infrared) spectral band.

2.4. Hydrological Data

Water levels of Longgan Lake were controlled by artificial regulation using three hydrological stations (Figure 1). Since the start of the wet season (usually from May to September), the gates are closed to store water in the lakes and prevent flooding of the land. The water is released back into the Yangtze River in late autumn [39]. Daily water level data (meters above sea level, reference to Wusong datum) from May to September each year from 1987 to 2018 were collected. In this study, the spring water level was defined as the the average water level in May, and the summer water level was defined as the average water level in June, July and August. However, spring and summer water levels were missing in some years due to incomplete water level records.

The fifth generation ECMWF atmospheric reanalysis of the global climate (ERA5) from 1987 to 2018 were used to analyze the temporal trend of annual precipitation for Longgan Lake. ERA5 provides several improvements compared to ERA-Interim data with a much higher resolution in both time and space [40]. Its horizontal resolution is approximately 30 km.

2.5. Methods

2.5.1. Determination of Lake Boundaries

The spectral signatures of aquatic vegetation largely overlap with the signatures of terrestrial vegetation, which leads to the misclassification of aquatic and terrestrial vegetation patches in their transitional areas. Thus, terrestrial areas around the lake were blocked out using a mask of the lake based on the water surface in 2018. The same mask was applied to all Landsat images to obtain comparable results. Moreover, the northeastern and southern boundary of the lake have also been masked, because these area have been extensively used for aquaculture.

2.5.2. Aquatic Vegetation Mapping

Large-scale aquatic vegetation mapping usually employs a series of spectral indices (SIs), combining with threshold determination approaches [41,42]. The performance of different SIs have been assessed for aquatic vegetation mapping, and the 2-band enhanced vegetation index (EVI2) outperforms others in extracting floating and emergent vegetation [20,21,43]. EVI2 is a two-band adaptation of EVI that has been developed without a blue band. It retains sensitivity and linearity as EVI in high biomass regions [44]. EVI2 is calculated based on Equation (1),

$$\mathrm{EVI2} = 2.5\frac{(R_{\mathrm{NIR}} - R_{\mathrm{R}})}{(R_{\mathrm{NIR}} + 2.4R_{\mathrm{R}} + 1)} \quad (1)$$

where R_{NIR} and R_{R} are the top-of-atmosphere (TOA) reflectance of the near-infrared and red bands.

EVI2 values were then used to distinguish between water and aquatic vegetation through a threshold selection method. Dynamic thresholds, instead of a static threshold, are normally recommended for remote sensing data of different phases, due to different satellite instruments used, or different atmospheric conditions or water environment for images of different dates [23,45]. For each scene, a threshold was selected based on the EVI2 histogram using the Otsu method that divide the study area into two classes (aquatic vegetation and open water) [46]. Otsu is a nonparametric unsupervised method, which find the threshold to minimize the within class variance of two classes. The histograms of EVI2 for 1997, 2001, and 2018 are shown in Figure 4 with the threshold values. For this study, the pixels with EVI2 values below and above the selected threshold were assigned as water and aquatic vegetation, respectively. The classification results and the false color composite images are also shown in Figure 4 for visual comparison.

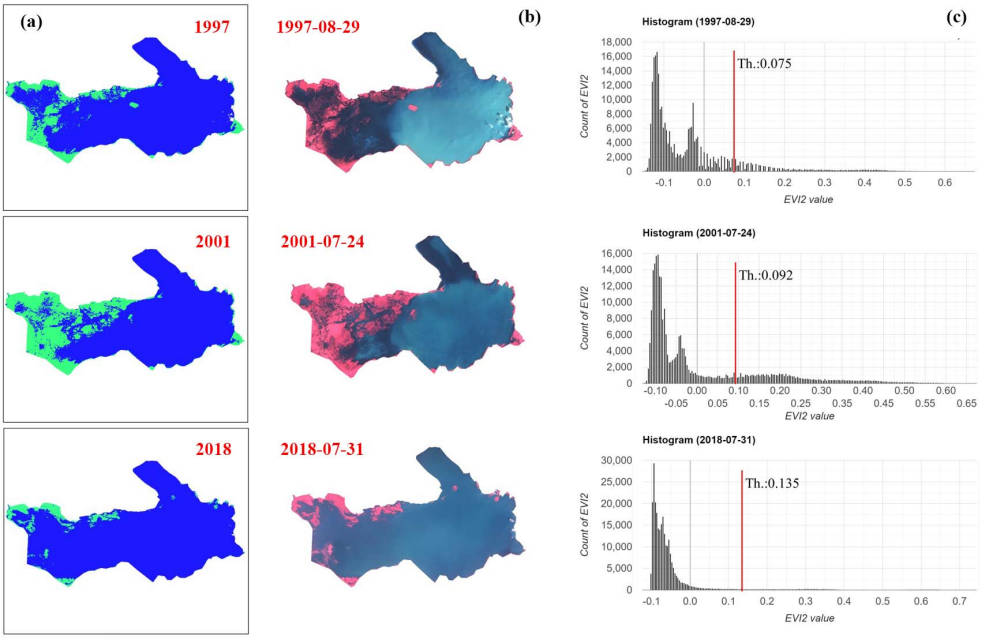

Figure 4. Classification results based on the optimized threshold for 1997, 2001, 2018. The pixels with EVI2 values below and above the selected threshold were assigned as water and aquatic vegetation, respectively. (**a**) Classification results; (**b**) The false color composite images; (**c**) EVI2 histogram and the Otsu segmentation thresholds.

2.5.3. Accuracy Assessment of Macrophytes Mapping

Extensive field survey data of aquatic vegetation in Longgan Lake were only available for September 2017 and September 2018 (Figure 3). The field survey results for a total of 48 field survey samples (pixels) were extracted and compared with the classification results of July 2017 and 2018, as shown in Figure 5 and Table 2. There were two possible reasons for the relatively low accuracy. Firstly, aquatic vegetation extent declined from summer to fall due to withering (e.g., *Trapa litwinowii* located in the center of the western lake withered from July to September). Secondly, floating macrophytes could change location quickly due to winds (e.g., *Eichhornia crassipes* located along the western shore of the lake during the survey of 2018 were not presented in the July image used for classification).

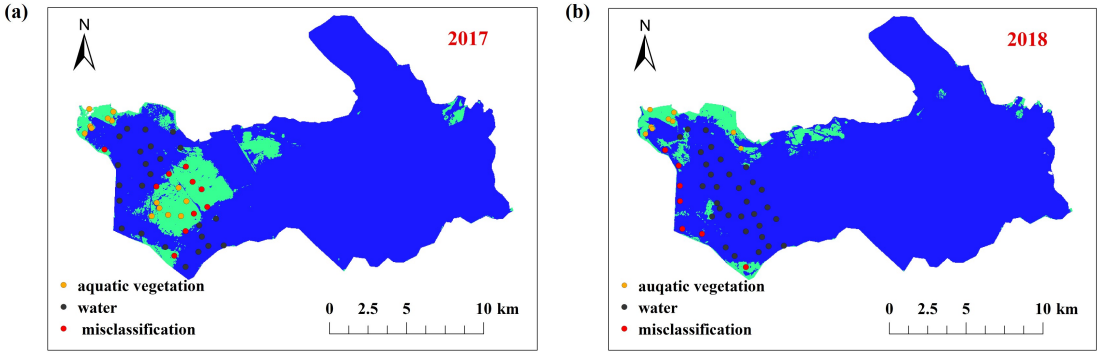

Figure 5. Comparison of field survey data and classification results for (**a**) 2017 and (**b**) 2018.

Table 2. Confusion matrix of classification result for aquatic vegetation (compared to field data).

Year	Overall Accuracy (%)	Kappa	Producer's Accuracy (%)	User's Accuracy (%)
2017	79.17	0.5833	100.00	58.33
2018	85.42	0.7267	60.00	90.00

Considering there was a two month difference between the Landsat data and the field data used, Sentinel-2 false color composite images of 26 July 2017 and 31 July 2018 were also used to validate the classification results. Aquatic vegetation boundaries were identified manually from Sentinel-2. Then, the manually delineated aquatic vegetation boundaries were compared with the classification results of Landsat using the confusion matrix. Table 3 listed the accuracy of aquatic vegetation classification. The results showed that the overall accuracies were higher than 90% and the kappa coefficients all exceeded 0.8, which demonstrated that the model performed well for distinguishing aquatic vegetation.

Table 3. Confusion matrix of classification result for aquatic vegetation (Compared to Sentinel-2).

Year	Overall Accuracy (%)	Kappa	Producer's Accuracy (%)	User's Accuracy (%)
2017	97.12	0.8682	83.04	94.62
2018	97.95	0.8183	82.75	83.10

3. Results

3.1. Seasonal and Decadal Variation of Water Level

The mean and variation of the monthly water level (meters above the sea water, reference to Wusong datum) for the study period were shown in Figure 6. It can be seen that the monthly average water level has been increasing, reaching its peak in August. Annual precipitation, average spring water level and summer water level of Longgan Lake from 1987 to 2018 were shown in Figure 7. Data gaps are caused by the lack of data. In spring, the highest water level was 13.49 m in 2010, and the lowest water level was 12.11 m in 2004. In summer, the highest water level was 16.28 m in 1992, and the lowest water level was 12.31 m in 2007. The changes of water level were generally consistent with the annual precipitation of Longgan Lake from 1987 to 2018. It can be seen that years of 1991, 1998, 2002, 2010, 2015 and 2016 have abnormally high annual precipitation and years of 2006 and 2007 have abnormally low annual precipitation.

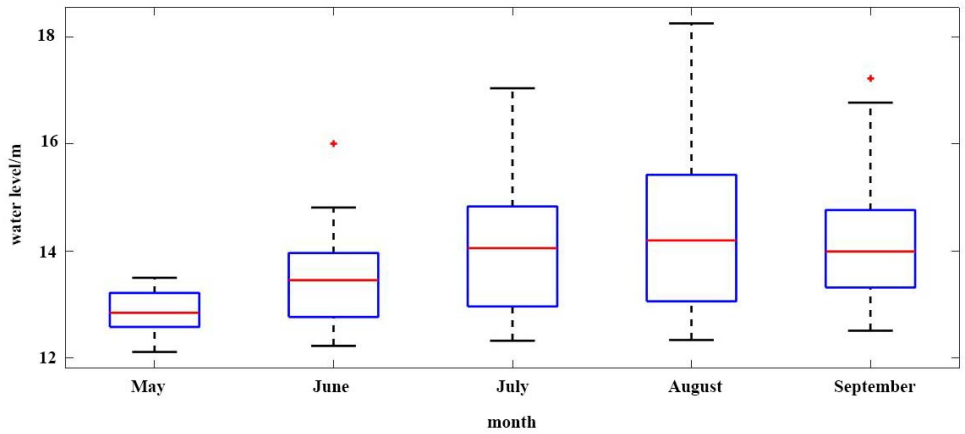

Figure 6. Box plot of the water levels from May to September for Longgan Lake (meters above sea level, reference to Wusong datum).

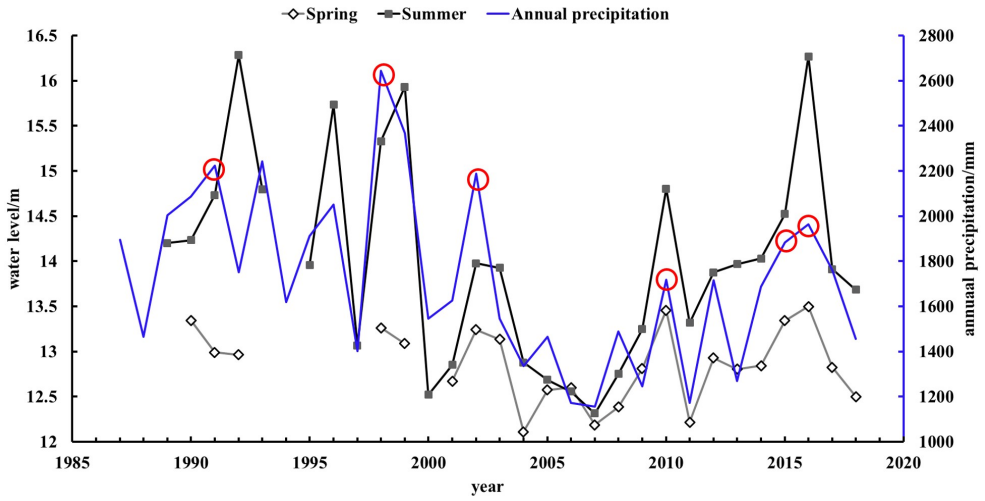

Figure 7. Annual precipitation, average spring water level and summer water level of Longgan Lake from 1987 to 2018. The red circles present years with abnormally high annual precipitation.

3.2. Inter-Annual Dynamics of Aquatic Vegetation

The spatial distribution of aquatic vegetation in Longgan Lake at the peak of vegetation coverage each year from 1987 to 2019 was shown in Figure 8. Due to the low temporal resolution of Landsat and the effects of cloud cover, it was impossible to accurately obtain the maximum aquatic vegetation coverage of each year. Even though the spatial distribution patterns of aquatic vegetation varied from year to year, aquatic vegetation were primarily distributed in the western region of the lake, where lake bottom elevation ranged from 11 to 12 m, with average water depth of less than 1 m in spring. For years that had high vegetation extent, aquatic vegetation expanded towards the center of the lake. For years with low vegetation extent, aquatic vegetation shrank towards the northwest corner.

The temporal variation of aquatic vegetation area in Longgan Lake from 1987 to 2019 were shown in Figure 9. In 2011, the vegetation area reached the maximum area of 73.99 km^2. In 2015, the vegetation area was the smallest, occupying 8.72 km^2, only about one-tenth of the aquatic vegetation area in 2011. In order to analyze the vegetation restoration process in a certain period under the influence of abnormal precipitation, the years of 1991, 1998, 2002, 2010 and 2015 were used as the dividing points. Thus, the inter-annual aquatic vegetation variation were divided into six stages. During the first stage (1987–1991), the vegetation area had remained above 35 km^2 in the first three years and then had decreased. Especially, the area was smallest in 1991, occupying only 14.87 km^2. The second stage occurred from 1992 to 1998. During this stage, the area began to increase, reaching to a maximum in 1996. Since then, the area had decreased, but at a lower rate. The third stage occurred from 1999 to 2002. During this period, the area increased firstly and then decreased. During the fourth stage (2003–2010), the area maintained at a higher value over 65 km^2. In 2010, the area dropped sharply to 12.34 km^2. During the fifth stage (2011–2015), the area increased firstly at a very high rate in 2011, and then remained above 45 km^2. In 2015, the area dropped sharply to 8.72 km^2. The sixth stage occurred from 2016 to 2019. During this stage, the area was very small except for 2019.

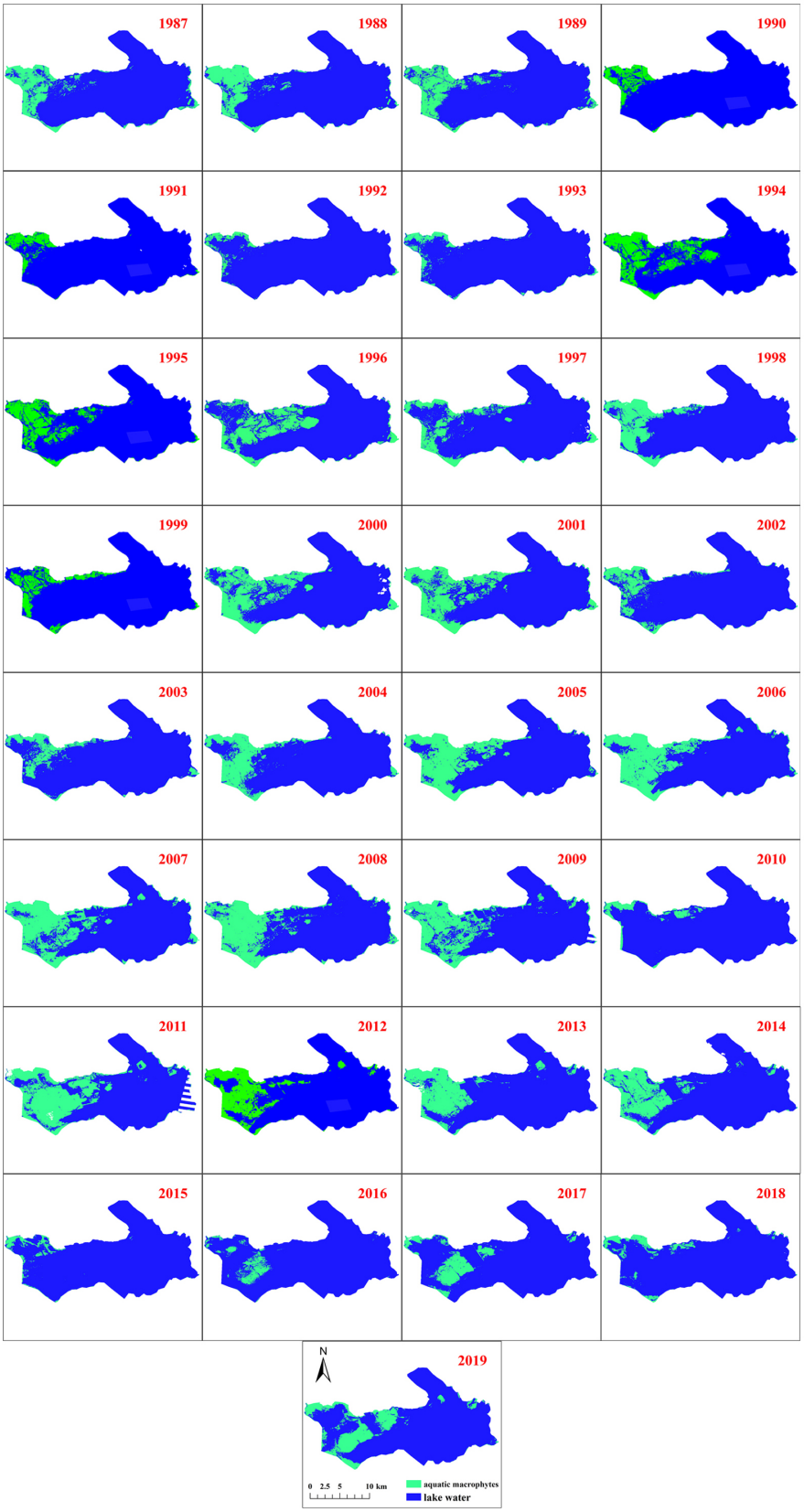

Figure 8. Spatial distribution map of aquatic vegetation in Longgan Lake from 1987 to 2019.

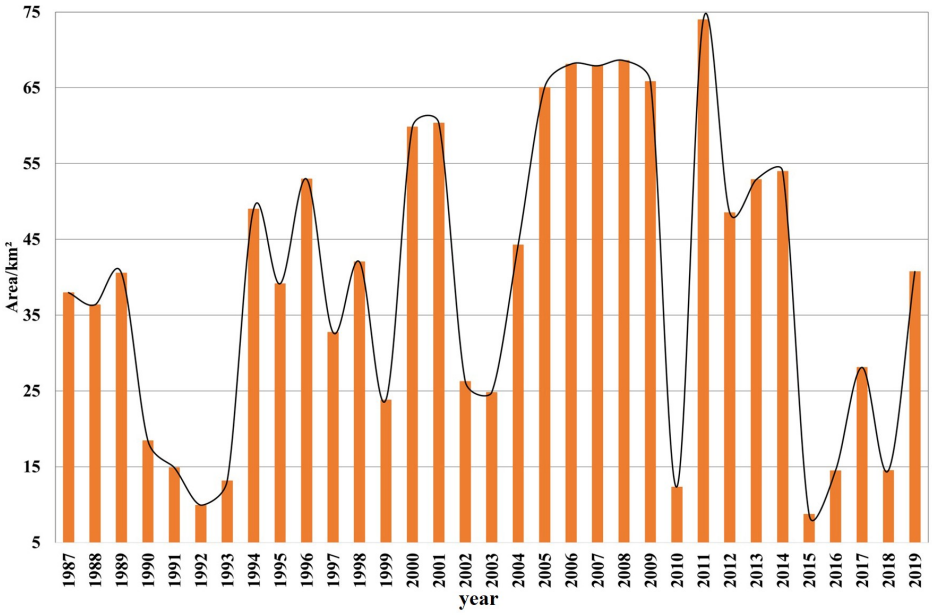

Figure 9. Aquatic vegetation area of Longgan Lake from 1987 to 2019.

3.3. Relationship between Aquatic Vegetation Area and Water-Level Change

The variation of aquatic vegetation area and water level for Longgan Lake from 1987 to 2019 were shown in Figure 10. When the water level rose above to 13 m in spring, the area of aquatic vegetation greatly reduced. When the water level exceeded 16 m in summer, the area decreased dramatically.

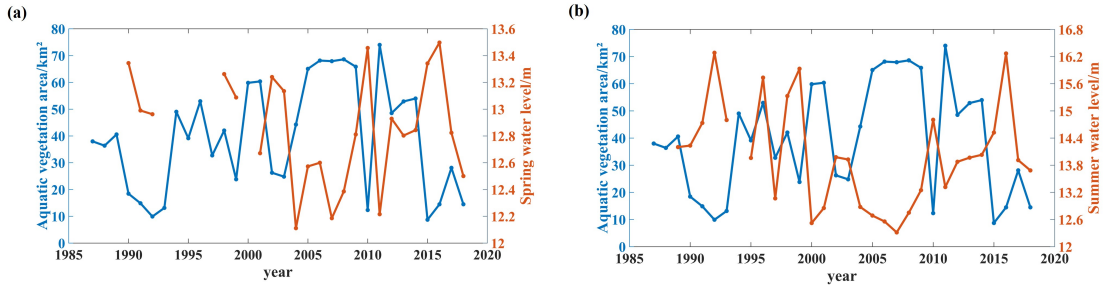

Figure 10. Decadal variations of aquatic vegetation area and water level for Longgan Lake from 1987 to 2019. (**a**) Aquatic vegetation area related to water level in spring; (**b**) Aquatic vegetation area related to water level in summer.

In order to explore the coupling relationship between the area of aquatic vegetation and water-level fluctuation rhythm, Pearson correlation analysis was used. The results revealed that aquatic vegetation area had a significant negative correlation with spring water level and summer water level, with Pearson correlation coefficients of -0.70 ($P < 0.01$) and -0.67 ($P < 0.01$), respectively. As shown in Figure 11, specifically, the area of aquatic vegetation was very large when water level was low, and vice versa. In 2011, the area of aquatic vegetation was largest, the spring water level was below 12.5 m and the summer water level was below 14 m.

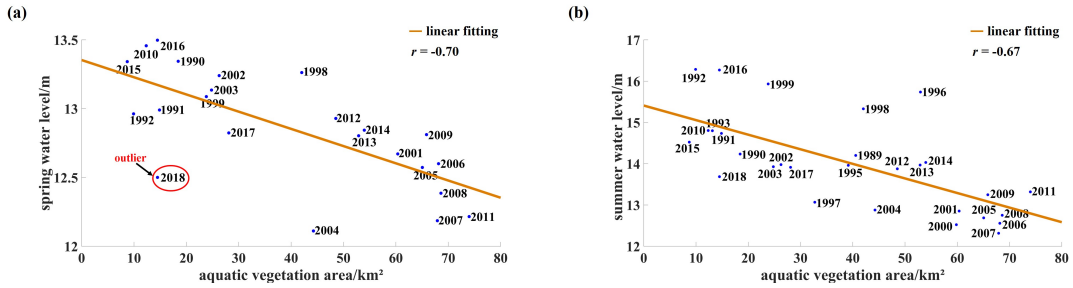

Figure 11. Correlation between aquatic vegetation distribution area and water level. (**a**) Spring water level; (**b**) Summer water level.

4. Discussion

4.1. Effects of Remote-Sensing Imagery Acquisition Time on the Maximum Aquatic Vegetation Area of a Year

According to field surveys, the main growth season for aquatic vegetation in Longgan Lake is from May to September. Thus, aquatic vegetation area normally reaches the maximum in late July. Therefore, July images were used with priority to get the maximum vegetation cover of a year. However, the maximum aquatic vegetation area extracted in this analysis might not be the true maximum cover area of a year. Firstly, images in June and August were used as supplements due to cloud coverage in July. Moreover, the locations of floating vegetation were greatly influenced by wind speed and direction, leading to large variability in their spatial distribution. As shown in Figure 11, some outliers did not follow the rule that the vegetation area was larger when the water level was lower. In 2018, the aquatic vegetation area was 14.49 km^2, and the water level in spring was 12.5 m. It showed that the water level in spring was low, but the extracted vegetation area was also relatively small compared to other years. As it can be seen in the PROBA-V image and Sentinel-2 image (Figure 12), large area of aquatic vegetation were distributed in the center of the western lake on 26 June 2018. However, these aquatic vegetation disappeared in the July 2018 images. Based on the field survey of 2017, the center of the western lake was largely covered by *Trapa litwinowii* + *Eichhornia crassipes* + *Spirodela polyrhiza* Ass. Same floating-leaved and floating plants present in June 2018, were possibly withered or blown away to other locations in July 2018. Despite these uncertainties, a good relationship between aquatic vegetation area and water level was still achieved for the three decades study period, indicating the robustness of the analysis.

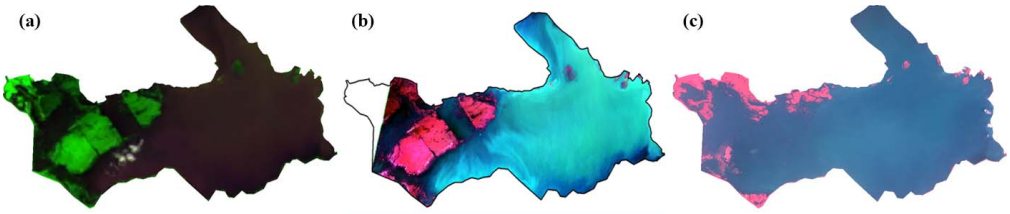

Figure 12. Comparison of PROBA-V image, Sentinel-2 image and Landsat 8 image in 2018. (**a**) PROBA-V image on 26 June 2018; (**b**) Sentinel-2 image on 26 June 2018; (**c**) Landsat 8 image on 31 July 2018.

4.2. Effects of Water-Level Fluctuation on Aquatic Vegetation Area

As shown in Figures 10 and 11, aquatic vegetation area showed a significant negative correlation with water level. The existing vegetation types in the lake have adapted to the long-term variation of water level. The expansion and retreat of aquatic vegetation are greatly related to lake bottom topography, as water depth is the determining factor for aquatic vegetation growth. The normal spring water depth in the northwestern part of the lake is less than 1 m, which is suitable for aquatic vegetation growth. For years with abnormally high spring water level, due to high water depth, aquatic vegetation retreated to areas close to the boundary of the lake where water depth was low.

When water level rose above to 13 m in spring and 16 m in summer, aquatic plants largely disappeared. To show the optimal water depth for aquatic vegetation, the distributions of spring and summer water depths for all area mapped as aquatic vegetation in all years were calculated. It can be seen in Figure 13 that in areas with aquatic vegetation, water depths did not exceed 2.5 m in May and 5 m in summer. To preserve aquatic vegetation in the western part of the lake, it is recommended that water depth remain close to 1 m in spring and close to 3 m in summer. In spring, higher water level reduced light, which was not conducive to seed germination and seedling growth [47,48]. In summer, continuous high water level could drown vegetation, resulting in reduced oxygen supplies and causing the death of aquatic plants [49]. Significantly, extreme hydrological events in summer, such as flooding, would cause massive aquatic vegetation collapse, and consequently the decline of ecosystem diversity.

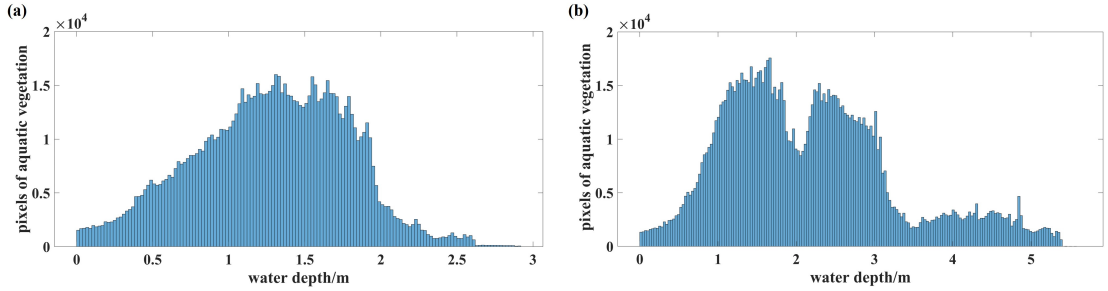

Figure 13. Water depth distribution for areas with aquatic vegetation in (**a**) Spring (average water depth in May) and (**b**) Summer (average water depth of June, July and August) for all years.

5. Conclusions

The aim of this study was to map the long term variability of aquatic vegetation extent in a human dammed lake and to investigate the correlation between aquatic vegetation and water level fluctuation of the lake. For this purpose, the modified enhanced vegetation index with Otsu threshold method was used to map the aquatic vegetation area in Longgan Lake for the 33-year period, including emerged, floating-leaved and floating macrophytes, using archived Landsat images from 1987 to 2019 on GEE platform. The classification results were validated by field survey data and other satellite data. Results showed that aquatic vegetation were mainly distributed in the western part of the lake, where lake bottom elevation ranged from 11 to 12 m, with average water depth close to 1 m in spring. The relationships between aquatic vegetation area and spring and summer water-level fluctuation were also analyzed. For years with increased vegetation cover, aquatic vegetation would expand from the northwestern to the center of the lake. Years with extremely high precipitation were related to low vegetation area. In the following years, the area normally restored. The aquatic vegetation area showed a significant negative correlation with the spring water level and summer water level. The results showed that aquatic vegetation was negatively affected when water depth exceeded 2.5 m in May and 5 m in summer. It is recommended that water depth remain close to 1 m in spring and close to 3 m in summer to assure successful aquatic vegetation growth. The results from our study provided information about the optimum water level for aquatic vegetation growth in Longgan Lake. These findings can provide the basis for wetland management and restoration. Future work will mainly focus on the classification of different aquatic vegetation types and the inter-seasonal dynamics based on multi-temporal and multi-source remote sensing imagery.

Author Contributions: S.Y. had the original idea for the study. G.Y. provided the methodology. W.T. and J.X. were responsible for analyzing the data and writing the paper. Y.J. offered background data about Longgan Lake. S.Y. and G.Y. supervised the research and provided valuable suggestions for the revision. S.Y., W.T. and Y.J. offered measured samples to validate our classification results in this paper. W.T., J.X. and Y.J. had significant contribution in coding and visualization. P.S. collected and analyzed the field data. All authors have read and agreed to the published version of the manuscript.

Funding: This work was supported by the National Natural Science Foundation of China under grants 31670464 and 41506208, partially by the Fundamental Research Funds for the Central Universities under Grant CCNU19TD002, CCNU18ZDPY03 and CCNU19TS001.

Acknowledgments: We would like to thank the staffs from the Bureau of Longgan Lake national nature reserve, Hubei, China for their assistance with fieldwork and their supports in this research. We also sincerely thank Jun Xu of Institute of Hydrobiology, Chinese Academy of Sciences , China for providing the topographic map of Longgan Lake. We also thank the anonymous reviewers for their insightful comments and suggestions, which lead to great improvements to the manuscript.

Conflicts of Interest: The authors declare no conflicts of interest.

References

1. Horppila, J.; Nurminen, L. Effects of submerged macrophytes on sediment resuspension and internal phosphorus loading in Lake Hiidenvesi (southern Finland). *Water Res.* **2003**, *37*, 4468–4474. [CrossRef]
2. Li, D.; Wang, L.; Ding, J. Ecological functions and resource utilization of aquatic plants. *Wetl. Sci.* **2011**, *9*, 290.
3. Phiri, C.; Chakona, A.; Day, J.A. Aquatic insects associated with two morphologically different submerged macrophytes, Lagarosiphon ilicifolius and Vallisneria aethiopica, in small fishless ponds. *Aquat. Ecol.* **2011**, *45*, 405–416. [CrossRef]
4. Zhang, Y.; Jeppesen, E.; Liu, X.; Qin, B.; Shi, K.; Zhou, Y.; Thomaz, S.M.; Deng, J. Global loss of aquatic vegetation in lakes. *Earth-Sci. Rev.* **2017**, *173*, 259–265. [CrossRef]
5. Guo, L. Doing battle with the green monster of Taihu Lake. *Science* **2007**, *317*, 1166. [CrossRef] [PubMed]
6. Sand-Jensen, K.; Riis, T.; Vestergaard, O.; Larsen, S.E. Macrophyte decline in Danish lakes and streams over the past 100 years. *J. Ecol.* **2001**, *88*, 1030–1040. [CrossRef]
7. Short, F.T.; Kosten, S.; Morgan, P.A.; Malone, S.; Moore, G.E. Impacts of climate change on submerged and emergent wetland plants. *Aquat. Bot.* **2016**, *135*, 3–17. [CrossRef]
8. Nõges, T.; Nõges, P. The effect of extreme water level decrease on hydrochemistry and phytoplankton in a shallow eutrophic lake. *Hydrobiologia* **1999**, *408*, 277–283. [CrossRef]
9. Geest, G.V.; Wolters, H.; Roozen, F.; Coops, H.; Roijackers, R.; Buijse, A.; Scheffer, M. Water-level fluctuations affect macrophyte richness in floodplain lakes. *Hydrobiologia* **2005**, *539*, 239–248. [CrossRef]
10. Yang, J.; Li, E.; Cai, X.; Wang, Z.; Wang, X. Research progress in response of plants in wetlands to water level change. *Wetl. Sci.* **2014**, *12*, 807–813.
11. Keddy, P.; Reznicek, A. Great Lakes vegetation dynamics: The role of fluctuating water levels and buried seeds. *J. Great Lakes Res.* **1986**, *12*, 25–36. [CrossRef]
12. Wilcox, D.A.; Nichols, S.J. The effects of water-level fluctuations on vegetation in a Lake Huron wetland. *Wetlands* **2008**, *28*, 487–501. [CrossRef]
13. Zhang, X.; Liu, X.; Wang, H. Effects of water level fluctuations on lakeshore vegetation of three subtropical floodplain lakes, China. *Hydrobiologia* **2015**, *747*, 43–52. [CrossRef]
14. Zhao, D.; Jiang, H.; Cai, Y.; An, S. Artificial regulation of water level and its effect on aquatic macrophyte distribution in Taihu Lake. *PLoS ONE* **2012**, *7*, e44836. [CrossRef] [PubMed]
15. Wang, M.; Liu, Z.; Luo, F.; Lei, G.; Li, H. Do amplitudes of water level fluctuations affect the growth and community structure of submerged macrophytes? *PLoS ONE* **2016**, *11*, e0146528. [CrossRef] [PubMed]
16. Oyama, Y.; Matsushita, B.; Fukushima, T. Distinguishing surface cyanobacterial blooms and aquatic macrophytes using Landsat/TM and ETM + shortwave infrared bands. *Remote Sens. Environ.* **2015**, *157*, 35–47. [CrossRef]
17. Liu, X.; Zhang, Y.; Shi, K.; Zhou, Y.; Tang, X.; Zhu, G.; Qin, B. Mapping aquatic vegetation in a large, shallow eutrophic lake: A frequency-based approach using multiple years of MODIS data. *Remote Sens.* **2015**, *7*, 10295–10320. [CrossRef]
18. Luo, J.; Li, X.; Ma, R.; Li, F.; Duan, H.; Hu, W.; Qin, B.; Huang, W. Applying remote sensing techniques to monitoring seasonal and interannual changes of aquatic vegetation in Taihu Lake, China. *Ecol. Indic.* **2016**, *60*, 503–513. [CrossRef]
19. Liang, Q.; Zhang, Y.; Ma, R.; Loiselle, S.; Li, J.; Hu, M. A MODIS-based novel method to distinguish surface cyanobacterial scums and aquatic macrophytes in Lake Taihu. *Remote Sens.* **2017**, *9*, 133. [CrossRef]

20. Villa, P.; Pinardi, M.; Tóth, V.; Hunter, P.; Bolpagni, R.; Bresciani, M. Remote sensing of macrophyte morphological traits: Implications for the management of shallow lakes. *J. Limnol.* **2017**, *76*, 109–126. [CrossRef]
21. Villa, P.; Pinardi, M.; Bolpagni, R.; Gillier, J.M.; Zinke, P.; Nedelcuţ, F.; Bresciani, M. Assessing macrophyte seasonal dynamics using dense time series of medium resolution satellite data. *Remote Sens. Environ.* **2018**, *216*, 230–244. [CrossRef]
22. Szabó, L.; Deák, B.; Bíró, T.; Dyke, G.J.; Szabó, S. NDVI as a Proxy for Estimating Sedimentation and Vegetation Spread in Artificial Lakes—Monitoring of Spatial and Temporal Changes by Using Satellite Images Overarching Three Decades. *Remote Sens.* **2020**, *12*, 1468. [CrossRef]
23. Lopes, C.L.; Mendes, R.; Caçador, I.; Dias, J.M. Evaluation of long-term estuarine vegetation changes through Landsat imagery. *Sci. Total Environ.* **2019**, *653*, 512–522. [CrossRef] [PubMed]
24. Gorelick, N.; Hancher, M.; Dixon, M.; Ilyushchenko, S.; Thau, D.; Moore, R. Google Earth Engine: Planetary-scale geospatial analysis for everyone. *Remote Sens. Environ.* **2017**, *202*, 18–27. [CrossRef]
25. Wang, X.; Xiao, X.; Zou, Z.; Hou, L.; Qin, Y.; Dong, J.; Doughty, R.B.; Chen, B.; Zhang, X.; Chen, Y.; et al. Mapping coastal wetlands of China using time series Landsat images in 2018 and Google Earth Engine. *ISPRS J. Photogramm. Remote Sens.* **2020**, *163*, 312–326. [CrossRef] [PubMed]
26. Wang, Y.; Ma, J.; Xiao, X.; Wang, X.; Dai, S.; Zhao, B. Long-term dynamic of Poyang Lake surface water: A mapping work based on the google earth engine cloud platform. *Remote Sens.* **2019**, *11*, 313. [CrossRef]
27. Inman, V.L.; Lyons, M.B. Automated Inundation Mapping Over Large Areas Using Landsat Data and Google Earth Engine. *Remote Sens.* **2020**, *12*, 1348. [CrossRef]
28. Hu, Y.; Huang, J.; Du, Y.; Han, P.; Wang, J.; Huang, W. Monitoring wetland vegetation pattern response to water-level change resulting from the Three Gorges Project in the two largest freshwater lakes of China. *Ecol. Eng.* **2015**, *74*, 274–285. [CrossRef]
29. Liang, D.; Lu, J.; Chen, X.; Liu, C.; Lin, J. An investigation of the hydrological influence on the distribution and transition of wetland cover in a complex lake floodplain system using time-series remote sensing and hydrodynamic simulation. *J. Hydrol.* **2020**, *587*, 125038. [CrossRef]
30. Tan, Z.; Jiang, J. Spatial-Temporal Dynamics of Wetland Vegetation Related to Water Level Fluctuations in Poyang Lake, China. *Water* **2016**, *8*, 397. [CrossRef]
31. Wan, R.; Xue, D.; David, S. Vegetation Response to Hydrological Changes in Poyang Lake, China. *Wetlands* **2019**, *39*, 99–112. [CrossRef]
32. You, H.; Fan, H.; Xu, L.; Wu, Y.; Wang, X.; Liu, L.; Yao, Z.; Yan, B. Effects of Water Regime on Spring Wetland Landscape Evolution in Poyang Lake between 2000 and 2010. *Water* **2017**, *9*, 467. [CrossRef]
33. Zhang, C.; Yuan, Y.; Zeng, G.; Liang, J.; Guo, S.; Huang, L.; Hua, S.; Wu, H.; Zhu, Y.; An, H.; et al. Influence of hydrological regime and climatic factor on waterbird abundance in Dongting Lake Wetland, China: Implications for biological conservation. *Ecol. Eng.* **2016**, *90*, 473–481. [CrossRef]
34. Zhang, E.; Cao, Y.; Langdon, P.; Jones, R.; Yang, X.; Shen, J. Alternate trajectories in historic trophic change from two lakes in the same catchment, Huayang Basin, middle reach of Yangtze River, China. *J. Paleolimnol.* **2012**, *48*, 367–381. [CrossRef]
35. Hu, H.; Kang, H.; Gong, G.; Zhu, M.; Zheng, W.; Wu, F.; He, D.; Li, Z.; Geng, D. Biodiversity of winter waterbirds in Hubei, China. *Resour. Environ. Yangtze Basin* **2005**, *14*, 422–428.
36. Zhang, S.; Dou, H.; Jiang, J. Aquatic vegetation in Longgan Lake. *J. Lake Sci.* **1996**, *8*, 161.
37. Tomaselli, V.; Di Pietro, R.; Sciandrello, S. Plant communities structure and composition in three coastal wetlands in southern Apulia (Italy). *Biologia* **2011**, *66*, 1027. [CrossRef]
38. Phase 2 USGS Gap-Fill Algorithm. Available online: https://landsat.usgs.gov/sites/default/files/documents/L7SLCGapFilledMethod.pdf (accessed on 7 October 2018).
39. Yuan, L.; Liu, G.; Li, W.; Li, E. Seed bank variation along a water depth gradient in a subtropical lakeshore marsh, Longgan Lake, China. *Plant Ecol.* **2007**, *189*, 127–137. [CrossRef]
40. Hersbach, H.; Bell, B.; Berrisford, P.; Hirahara, S.; Horányi, A.; Muñoz-Sabater, J.; Nicolas, J.; Peubey, C.; Radu, R.; Schepers, D.; et al. The ERA5 global reanalysis. *Q. J. R. Meteorol. Soc.* **2020**. [CrossRef]
41. Hu, C. A novel ocean color index to detect floating algae in the global oceans. *Remote Sens. Environ.* **2009**, *113*, 2118–2129. [CrossRef]
42. Zhao, D.; Lv, M.; Jiang, H.; Cai, Y.; Xu, D.; An, S. Spatio-temporal variability of aquatic vegetation in Taihu Lake over the past 30 years. *PLoS ONE* **2013**, *8*, e66365. [CrossRef] [PubMed]

43. Villa, P.; Bresciani, M.; Bolpagni, R.; Pinardi, M.; Giardino, C. A rule-based approach for mapping macrophyte communities using multi-temporal aquatic vegetation indices. *Remote Sens. Environ.* **2015**, *171*, 218–233. [CrossRef]
44. Jiang, Z.; Huete, A.R.; Didan, K.; Miura, T. Development of a two-band enhanced vegetation index without a blue band. *Remote Sens. Environ.* **2008**, *112*, 3833–3845. [CrossRef]
45. Ji, L.; Zhang, L.; Wylie, B. Analysis of dynamic thresholds for the normalized difference water index. *Photogramm. Eng. Remote Sens.* **2009**, *75*, 1307–1317. [CrossRef]
46. Otsu, N. A threshold selection method from gray-level histograms. *IEEE Trans. Syst. Man Cybern.* **1979**, *9*, 62–66. [CrossRef]
47. Zhang, X.; Liu, X.; Wang, H. Developing water level regulation strategies for macrophytes restoration of a large river-disconnected lake, China. *Ecol. Eng.* **2014**, *68*, 25–31. [CrossRef]
48. Zou, L.; Nie, Z.; Yao, X.; Shi, J. Effects of light on submerged macrophytes in eutrophic water: Research progress. *Chin. J. Appl. Ecol.* **2013**, *24*, 2073–2080.
49. Yuan, S.; Zhang, X.; Liu, X.; Wang, H. Ecological water level management strategy for aquatic vegetation in the mid-lower yangtze shallow lakes. *Acta Hydrobiol. Sin.* **2019**, *43*, 104–109.